

Singlet–Triplet Splittings in CX₂ (X = F, Cl, Br, I) Dihalocarbenes via Negative Ion Photoelectron Spectroscopy

Rebecca L. Schwartz, Gustavo E. Davico, Tanya M. Ramond, and W. Carl Lineberger*

JILA, University of Colorado and National Institute of Standards and Technology, and Department of Chemistry and Biochemistry, University of Colorado, Boulder, Colorado 80309-0440

Received: June 29, 1999; In Final Form: August 9, 1999

The 364 nm negative ion photoelectron spectra of CF₂[−], CCl₂[−], CBr₂[−], and Cl₂[−] exhibit transitions to two different electronic states, the ¹A₁ and ³B₁. The CF₂[−] spectrum exhibits well-resolved transitions to both electronic states. In the cases of CCl₂[−], CBr₂[−], and Cl₂[−], the spectra exhibit extended, partially resolved vibrational progressions and the two states are overlapped, making a direct determination of the origin transition energy not possible. The overlapped spectra show that the singlet–triplet splittings in the heavier halocarbenes are much smaller than for CF₂[−]. The results of ab initio calculations have been used to generate Franck–Condon simulations of the spectra, which aid in the determination of the band origins. The ¹A₁ state is found to be the lower state for CF₂, CCl₂, and CBr₂ and the electron affinities have been determined to be 0.180 ± 0.020, 1.59 ± 0.07, and 1.88 ± 0.07 eV, respectively. For Cl₂, the triplet state is apparently the lower lying state with an electron affinity of 2.09 ± 0.07 eV. The singlet–triplet splitting energy has been determined to be 54 ± 3, 3 ± 3, 2 ± 3, −1 ± 3 kcal/mol for CF₂, CCl₂, CBr₂, and Cl₂, respectively. In addition, the bending and symmetric stretching vibrational frequencies have been determined for either one or both states.

I. Introduction

Carbenes have attracted a large amount of interest, both experimentally and theoretically, due to their importance as intermediates in many organic reactions. Of particular importance are the low-lying neutral singlet and triplet states, which have different chemical properties that affect their reactivity with various organic molecules.^{1–4} There have been many ab initio calculations that focus on both the singlet ¹A₁ and the triplet ³B₁ neutral states of the dihalocarbenes: CF₂, CCl₂, CBr₂, and Cl₂. Early calculations by Bauschlicher and co-workers aimed at determining the structure and energetics of simple carbenes including CF₂,⁵ CCl₂,⁵ and CBr₂.⁶ There were also two early calculations that predicted the electronic spectrum and vibrational frequencies of CCl₂.^{7,8} Carter and Goddard^{9–11} reported a thorough study of the singlet–triplet splittings (ΔE_{ST}) in the neutral dihalocarbenes. A great deal of effort was devoted to understanding the bonding of the halogen atoms to the carbon atom and the role it plays in determining the relative stabilities of the singlet and triplet states. Gutsev and Ziegler¹² published a study on both the anion and neutral states of the dihalocarbenes. These density functional calculations determined geometries, electron affinities, ΔE_{ST} , and dissociation energies. Russo et al.¹³ later calculated the geometries, ΔE_{ST} , and vibrational frequencies for the two low-lying neutral states using density functional computations at the linear combination of Gaussian-type-orbital local-spin-density level. Within the past five years, two other groups have focused on calculating ΔE_{ST} for the series of dihalocarbenes using the difference-dedicated configuration interaction method¹⁴ and Møller–Plesset perturbation theory.¹⁵ All of these calculations predict that the dihalocarbenes have a singlet ground state with the ³B₁ state lying 10–35 kcal/mol higher in energy for CCl₂, CBr₂, and Cl₂.

In addition to the long list of theoretical studies on CX₂ (X = F, Cl, Br, I), there have also been various experimental investigations. Most of the experiments on the dihalocarbenes have been performed on CF₂. Early electronic spectroscopy experiments determined the vibrational frequencies of CF₂(¹A₁).^{16–20} There have also been a number of infrared studies within matrix^{21,22} and gas-phase environments,^{23–27} as well as a microwave study²⁸ from which structures, frequencies, and lifetimes were obtained. Few studies have involved the triplet ³B₁ state of CF₂. Koda^{29,30} obtained an emission spectrum assigned to the CF₂(³B₁) → CF₂(¹A₁) intercombination transition; the vibrational distribution and relaxation of CF₂(³B₁) following the reaction of oxygen with tetrafluoroethylene was also characterized. It is from these experiments that the only experimental measurement of the singlet–triplet splitting in CF₂, 56.6 kcal/mol, was obtained. More recently, Huber and co-workers³¹ produced triplet CF₂ following the photodissociation of C₂F₄. Various experimental investigations have been carried out to characterize CCl₂^{32–39} and CBr₂^{39–45} in their ground ¹A₁ states. Both the geometries and vibrational frequencies have been determined. Squires and co-workers have performed various experimental and theoretical studies to determine the thermochemical properties of several carbenes including CF₂ and CCl₂.^{46,47} They found a correlation between the thermochemical quantities and the singlet–triplet energy splittings. Finally, 488 nm (2.54 eV) photoelectron spectra of CF₂[−] and CCl₂[−] were observed in this laboratory.⁴⁸ These spectra revealed the singlet states of CF₂ and CCl₂, from which the electron affinities and vibrational frequencies were obtained. The 2.54 eV photon energy did not access the triplet states of CF₂ and CCl₂. Similarly, the photoelectron spectra of CBr₂[−] and Cl₂[−] were not measured because of their high electron affinities. To our knowledge, no experiments have been performed to characterize the triplet states of CCl₂ or CBr₂. In addition, there are no experimental results on the Cl₂ dihalocarbene for either state.

* Corresponding author. Address for correspondence: JILA, University of Colorado, Campus Box 440, Boulder, CO 80309-0440. E-mail: wcl@jila.colorado.edu. Fax: (303) 492-8994.

This paper presents the results of photoelectron spectroscopy (PES) on CF_2^- , CCl_2^- , CBr_2^- , and Cl_2^- . Vibrational frequencies, origin transition energies, and singlet–triplet splittings for all of the dihalocarbenes are reported and compared to theoretical calculations.

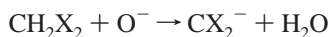
This paper contains a brief description of the experimental apparatus and procedure in section II. The results of the experiment are presented in section III, followed by a detailed discussion in section IV. Section V contains a summary of these results.

II. Experimental Section

The negative ion photoelectron spectrometer used in this experiment has been described in detail previously; therefore, only a brief description will be given here.⁴⁹ The spectrometer consists of three main regions: an ion source, a Wien filter, and an interaction region. The ion source includes a flowing afterglow region within which the negative ions are produced. Following collisional relaxation, the typical vibrational temperature of the ions is 300 K. The negative ions are extracted from the afterglow region, differentially pumped, and accelerated to 735 eV before being mass selected with a Wien filter. The mass-selected ions are decelerated to 38 eV before interacting with the 364 nm (3.408 eV) radiation from an Ar ion laser. The output of the laser is injected into an optical build-up cavity with approximately 100 W of circulating power within which it intersects the ion beam at a right angle. The kinetic energy of the photodetached electrons is monitored by a hemispherical energy analyzer positioned orthogonal to both the ion and laser beam axes. The electron energy resolution for each spectrum is approximately 12 meV.

The photoelectron spectra are recorded as a function of electron kinetic energy (eKE) and are subsequently converted to electron binding energy (eBE), where $\text{eBE} = h\nu - \text{eKE}$. Thus, electrons with high kinetic energy appear as peaks at the low end of the electron binding energy scale. The absolute electron energies of the spectra are calibrated using the well-known O^- transition at 1.461 110 3 eV as a reference.⁵⁰ A photoelectron spectrum of O^- is collected at the beginning of each day for calibration purposes. A small compression factor (<1%) of the energy scale is applied upon calibration. The compression factor is determined by comparing the positions of the transitions in a W^- spectrum, which span the entire energy scale, with the known values.⁵¹

In this experiment, the series of CX_2^- ($X = \text{F}, \text{Cl}, \text{Br}, \text{I}$) dihalocarbenes have been studied via photoelectron spectroscopy. Ions are formed via the H_2^+ abstraction reaction,⁵²



The O^- ions are generated by passing a mixture of approximately 0.5 Torr of He and O_2 through a microwave discharge into the flow tube. The CH_2X_2 is injected into the flowing afterglow region through an adjustable inlet so that the reaction with O^- can be optimized. Typical ion currents for CF_2^- , CCl_2^- , CBr_2^- , and Cl_2^- are between 20 and 35 pA. The production of the ions is optimized by varying the flows of the helium, oxygen, and CH_2X_2 and by moving the position of the inlet. All of the reagents have purities of at least 99%.

Photoelectron spectra were collected at three different laser polarizations angles, $\theta = 0^\circ$, 54.7° , and 90° , referred to as parallel, magic angle, and perpendicular, respectively. Here, θ is defined as the angle between the laser polarization of the incident light and the direction of the collected electrons. The

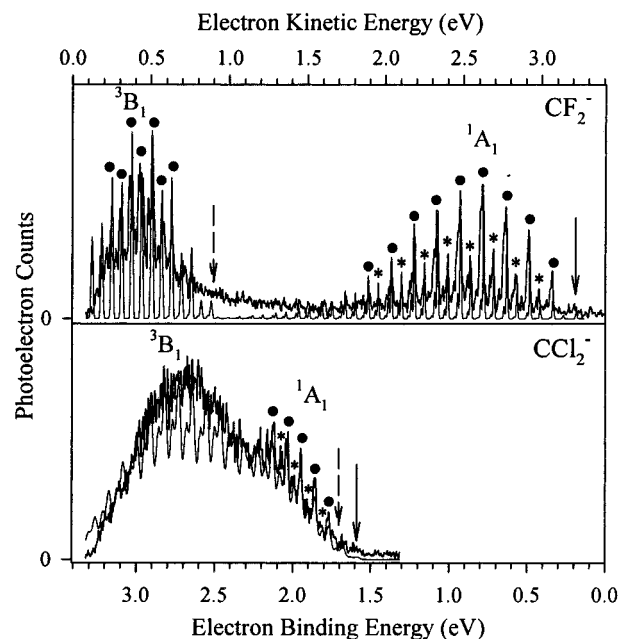


Figure 1. Negative ion photoelectron spectra of CF_2^- (top) and CCl_2^- (bottom) recorded at the magic angle, 54.7° (thick lines). The singlet $^1\text{A}_1$ and triplet $^3\text{B}_1$ states are present in both spectra; they are separated in CF_2 but overlapped in CCl_2 . Transitions that are attributed to the symmetric stretching vibration are marked \bullet and combination bands of one quantum of bend with a progression of the symmetric stretch are labeled $*$. The energies of the origin transitions determined from simulations (see text for details) in the singlet and triplet states are marked with a solid arrow and dashed arrow, respectively. In addition, a simulation (thin line) of each spectrum is shown.

photoelectron differential cross section is given by

$$\frac{d\sigma}{d\Omega} = \frac{\sigma_{\text{total}}}{4\pi} [1 + \beta P_2(\cos \theta)]$$

where σ_{total} is the total cross section, β is the asymmetry parameter,⁵³ and $P_2(\cos \theta) = (3 \cos^2 \theta - 1)/2$. The value of β ranges from -1 to $+2$. At the magic angle, 54.7° , $P_2(\cos \theta) = 0$ and the spectrum is independent of β .

In order to aid in the assignments of the photoelectron spectra and to generate simulations, ab initio calculations were carried out on the anion ground state and the singlet and triplet neutral states of all four dihalocarbenes. Both geometry optimization and frequency calculations were performed. All of the calculations were performed using the Gaussian 94 suite of programs⁵⁴ using second-order Møller–Plesset perturbation theory including all electrons (MP2 FULL). Spin-unrestricted wave functions were used for the open-shell species and there is no evidence of any significant spin contamination. The 6-311+G* basis set was used for CF_2 , CCl_2 , and CBr_2 in order to simplify comparisons among the systems. For Cl_2 , LanL2DZ as an effective core potential for the core electrons of the iodine atom was used and the valence electrons basis set coefficients were taken directly from Radom and co-workers.⁵⁵ However, our calculations include up until the d functions. The 6-31+G* basis set was used for the carbon atom in Cl_2 .

III. Results

A. Magic Angle. The 364 nm negative ion photoelectron spectra of the CX_2^- dihalocarbenes recorded at the magic angle are displayed in Figures 1 and 2 (thick lines). Each spectrum consists of transitions from the anion ground state ($^2\text{B}_1$) to both the singlet ($^1\text{A}_1$) and the triplet ($^3\text{B}_1$) CX_2 neutral states. Each

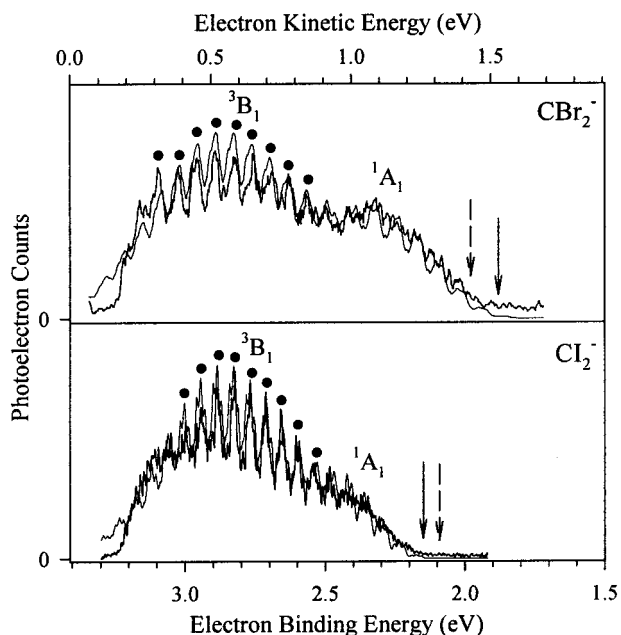


Figure 2. Negative ion photoelectron spectra of CBr_2^- (top) and Cl_2^- (bottom) recorded at the magic angle, 54.7° (thick lines). The singlet 1A_1 and triplet 3B_1 states are present in both spectra; however, they are considerably overlapped in energy. Transitions that are attributed to the symmetric stretching vibration in the triplet state of each spectra are marked \bullet . The energies of the origin transitions determined from simulations (see text for details) in the singlet and triplet states are marked with a solid arrow and dashed arrow, respectively. In addition, a simulation (thin line) of each spectrum is shown.

TABLE 1: Vertical Detachment Energies (VDE) of the Singlet and Triplet States^a

	CF_2	CCl_2	CBr_2	Cl_2
VDE				
singlet (1A_1)	0.90	2.17	2.34	2.43
triplet (3B_1)	2.96	2.67	2.81	2.83
$\Delta\text{VDE}_{\text{ST}}$	2.06	0.50	0.47	0.40

^a All values are in electronvolts. Error bars are 0.05 eV.

spectrum shows long vibrational progressions for both states due to the difference in the C–X bond length and the X–C–X bond angle between the anion and neutral geometries. There is a great deal of overlap between the singlet and triplet states except in the CF_2^- spectrum where there is an obvious separation between the states. In addition, it is difficult to identify the origin for each state except in the case of the CF_2 singlet state where a distinct feature can be assigned as the origin transition at 0.180 ± 0.020 eV, marked with a solid arrow in the top spectrum of Figure 1. The 364 nm radiation in this study allows for the observation of a larger energy range than the previous study using 488 nm.⁴⁸

Although most of the origin transitions cannot be identified, the vertical detachment energy (VDE), the energy at which the neutral CX_2 geometry is the same as the anion minimum energy configuration, can be obtained directly from the position of the maximum photoelectron signal. Both states in each spectrum have been fit with a Gaussian in order to obtain the VDE. The difference in the VDE of the singlet and triplet states ($\Delta\text{VDE}_{\text{ST}}$) provides only an approximation for the singlet–triplet splitting energy (ΔE_{ST}) as will be discussed in section IV.C. We define ΔE_{ST} as the difference between the origin transition energies that will lie to lower electron binding energy of the VDE in all cases. The individual VDEs are listed in Table 1 along with the $\Delta\text{VDE}_{\text{ST}}$. The most striking result is that the $\Delta\text{VDE}_{\text{ST}}$

decreases dramatically from about 2.0 eV for CF_2 to approximately 0.5 eV for CCl_2 , CBr_2 , and Cl_2 . This decrease in splitting is illustrated in Figures 1 and 2 where the states are well separated in the case of CF_2 and are overlapped for the other dihalocarbenes. A more detailed analysis of the singlet–triplet splittings including Franck–Condon calculations is discussed in section IV.C.

The CF_2^- spectrum in Figure 1 shows vibrational progressions that can be readily assigned. At low electron binding energy, the singlet state consists of a dominant progression that is attributed to the pure C–F symmetric stretching vibration. The smaller peaks are assigned to combination bands of the C–F symmetric stretching progression and one quanta of F–C–F bending vibration. Also present in the spectrum are combination bands that involve hot band transitions, which originate from the $\nu = 1$ level in the anion. Although the neutral states are slightly overlapped in the CCl_2^- photoelectron spectrum (bottom of Figure 1), the singlet state shows well-resolved progressions that can be assigned in a manner similar to the CF_2^- spectrum. At low electron binding energies, the main peaks correspond to a progression in the pure C–Cl symmetric stretching vibration (\bullet) while the indicated smaller peaks ($*$) are attributed to the C–Cl symmetric stretch with one quantum of Cl–C–Cl bending vibration. Assignments of individual peaks within the singlet states of the CBr_2^- and Cl_2^- photoelectron spectra are more difficult. As seen in Figure 2, the singlet states contain minimal vibrational structure and there is a considerable amount of overlap between the singlet and triplet states, and therefore no assignments have been made. An explanation and detailed analysis of these vibrational frequencies are given in Section IV.A.1.

Similar to the singlet state of CF_2 , the triplet state, which lies at high electron binding energy in Figure 1, shows vibrational progressions attributed to the pure C–F symmetric stretching vibration along with a progression of the symmetric stretch combined with the F–C–F bend. With the aid of theoretical calculations, the distinct peaks in the CBr_2^- and Cl_2^- photoelectron spectra are assigned to C–X (X = Br, I) symmetric stretching vibrations and bend–stretch combination bands within their respective triplet states. Unlike CF_2 , CBr_2 , and Cl_2 , the CCl_2 triplet state does not exhibit resolvable vibrational structure. A detailed discussion of this analysis is presented in Section IV.A.2.

B. Polarization Study and Angular Distributions. Photoelectron spectra of the CX_2^- dihalocarbenes collected at two other laser polarization angles relative to the direction of electron collection, $\theta = 0^\circ$ (parallel) and $\theta = 90^\circ$ (perpendicular), are displayed in Figure 3. The changes in the photoelectron spectra upon changing θ can be characterized quantitatively by determining the value of the asymmetry parameter, β , for each state

$$\frac{I_0 - I_{90}}{I_0 + I_{90}}$$

where I_0 is the intensity of a single peak at $\theta = 0^\circ$ and I_{90} is the intensity of the same peak at $\theta = 90^\circ$.

The angular distribution of the detached electron depends on the symmetry of the orbital from which it originated in the anion ground state. To better understand the angular distribution of the ejected electron and the effects it has on the photoelectron spectra, consider atomic photoelectron detachment.⁵³ Photodetachment of an s electron adds one unit of angular momentum from the photon resulting in an outgoing p-wave, with an angular

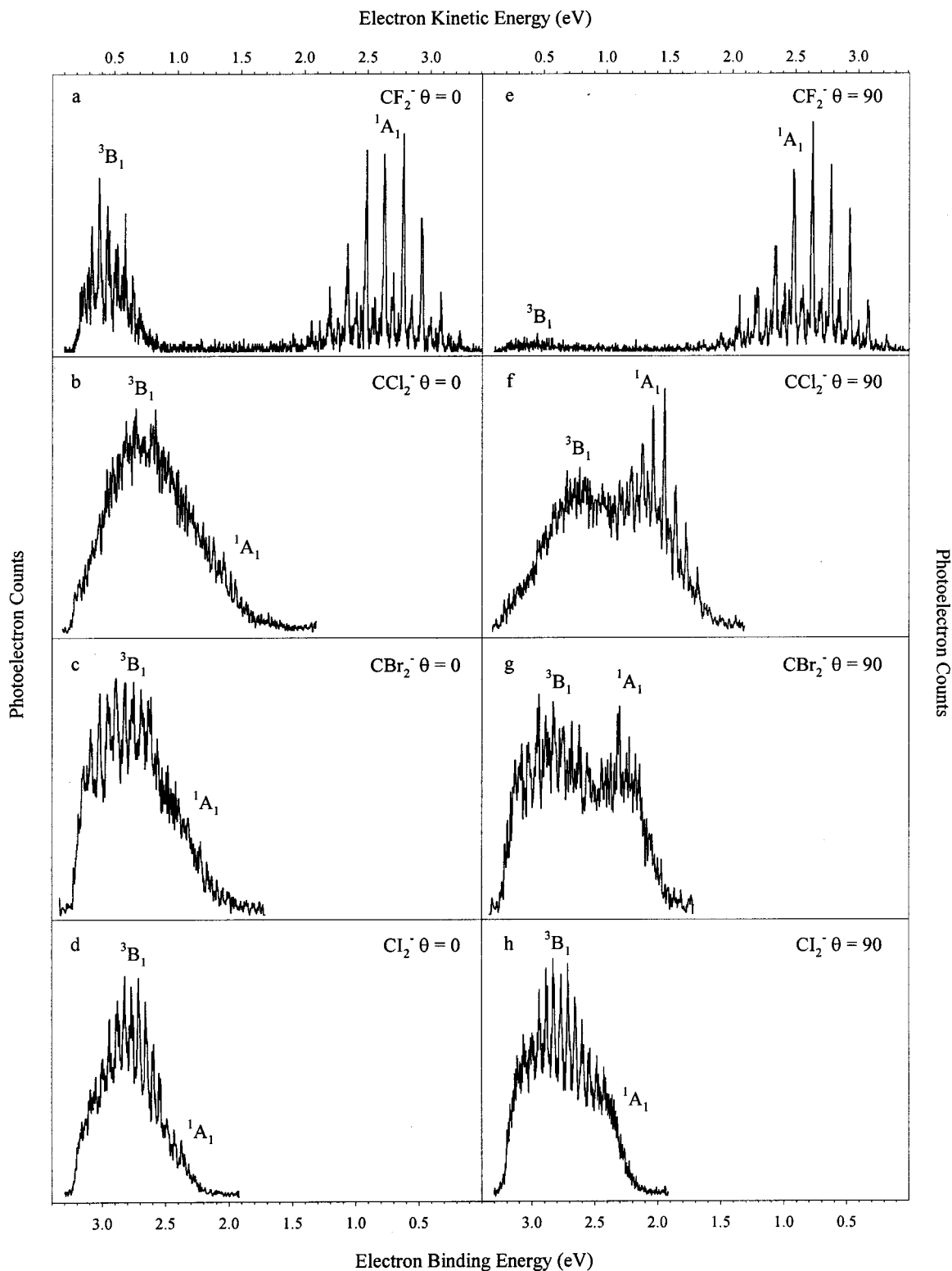


Figure 3. Negative ion photoelectron spectra of CF_2^- , CCl_2^- , CBr_2^- , and Cl_2^- recorded at laser polarizations, $\theta = 0^\circ$ and 90° with respect to the axis of electron detection. The difference in the spectra taken at orthogonal polarizations provides information on the orbitals from which the electrons originated and allows for the determination of the asymmetry parameter, β .

distribution that is independent of the electron kinetic energy and has a $\cos^2 \theta$ distribution with $\beta = 2$. An electron that originates from a p orbital in an atomic anion can have an outgoing s- or d-wave; the one unit of angular momentum from the photon either adds to or subtracts from the one unit of angular momentum of the electron. These two partial waves interfere giving an angular distribution that is a function of the electron kinetic energy. Near zero electron kinetic energy, the

lowest partial wave dominates giving an isotropic angular distribution and $\beta = 0$. As the electron kinetic energy increases toward 1 eV, β approaches -1 , a $\sin^2 \theta$ distribution. At even higher eKE (>1 eV) the value of β approaches 2.

For a molecule, the lack of spherical symmetry and the effects of rotational averaging make the understanding of the asymmetry parameter more complicated. In general, an electron that originates from an s-type orbital results in $\beta \sim 2$, a $\cos^2 \theta$

TABLE 2: Asymmetry Parameter, β , for Photodetachment of CF_2^- , CCl_2^- , CBr_2^- , and CI_2^- ^a

	CF_2	CCl_2	CBr_2	CI_2
singlet (1A_1)				
peak	2.64	1.46		
β^b	-0.4	-0.7	<0 ^c	<0 ^c
triplet (3B_1)				
peak	0.38	0.67	0.59	0.69
β^b	2.0	0.5	0.4	0.4

^a Peak positions are electron kinetic energies in electronvolts. ^b Error bars are 0.1. ^c Lack of structure in the singlet states and the overlap of the singlet and triplet states inhibit the determination of an accurate value for β .

distribution. An electron from a p-type orbital gives $\beta < 0$ and from a d-type orbital, $\beta = 0$.

Since transitions to a singlet versus a triplet state originate from different orbitals in the anion ground state, one would expect a difference in the peak direction of the detached electrons. Figure 3 shows the CF_2^- , CCl_2^- , CBr_2^- , and CI_2^- photoelectron spectra, which illustrate an obvious preference in photodetachment to the singlet and/or triplet states depending on the polarization of the incident laser light. There is a general trend that the singlet state preferentially detaches perpendicular to the laser polarization and the triplet state peaks parallel to the laser polarization. In the CF_2^- photoelectron spectrum recorded at $\theta = 0^\circ$ (Figure 3a), both the triplet and singlet states are present in equal proportions. At $\theta = 90^\circ$ (Figure 3e), however, there is only a hint of the triplet state present in the spectrum while the intensity of the singlet state is essentially the same as that measured in the $\theta = 0^\circ$ spectrum. In the CCl_2^- , CBr_2^- , and CI_2^- photoelectron spectra at $\theta = 0^\circ$ (Figure 3b–d), the triplet state is dominant with only a hint at the presence of the singlet state. It is clear that the presence of the singlet state decreases from CF_2 to CI_2 at parallel polarization. In contrast, there is significant detachment to *both* the singlet and triplet states of CCl_2 , CBr_2 , and CI_2 at $\theta = 90^\circ$ (Figure 3f–h).

These observations confirm that two different orbitals, each with different symmetry in the ground state of the anion, are involved in the transitions to the two observed states. Evaluating β for each state supports the singlet and triplet assignment of each electronic state. Due to spectral overlap and insufficient vibrational structure in the singlet state of CBr_2 and CI_2 , the β parameter could only be determined for CF_2 and CCl_2 with values of $\beta < 0$, indicating that the electron has been detached from a π orbital, resulting in the singlet state. For the triplet states, a β parameter could be obtained for each dihalocarbene. The values are all greater than zero, decreasing from 2.0 for CF_2 to 0.4 for CI_2 . The value of 2.0 suggests that the electron detachment occurs from a σ orbital in the anion, giving rise to the triplet state. As the halogen atom gets larger, it is less appropriate to describe the orbitals as purely σ or π . A more detailed explanation of the orbitals is found in section IV.D. The β values along with the electron kinetic energies of the peaks can be found in Table 2.

The spectra in Figure 3 are also used to separate the overlapping singlet and triplet states. The triplet state can be isolated from the singlet state through a subtraction scheme. After normalizing the spectra taken at $\theta = 90^\circ$ to those recorded at $\theta = 0^\circ$, the spectra are subtracted, resulting in a spectrum that is attributed mainly to transitions within the triplet state. These subtracted spectra were also fit with a Gaussian in order to determine the VDE of the triplet states. The values are in good agreement with those determined in section III.A and the differences in the fits are included in the error bars listed in Table 1.

TABLE 3: Bond Distances (r_{CX}) and Angles (θ_{XCX}) (X = F, Cl, Br, I) for All of the Dihalocarbenes in Both the Anion and Neutral States^a

	CF_2^b	CCl_2^b	CBr_2^b	CI_2^c
anion				
r_{CX}	1.44	1.87	2.05	2.25
θ_{XCX}	100.30	104.85	105.49	107.39
neutral singlet				
r_{CX}	1.30	1.71	1.88	2.09
θ_{XCX}	104.91	110.36	110.66	112.66
neutral triplet				
r_{CX}	1.32	1.68	1.84	2.03
θ_{XCX}	119.16	127.52	129.27	132.21

^a All values are taken from MP2 level Gaussian 94 calculations using the indicated basis set. Distances are in angstroms and angles are in degrees. ^b 6-311+G*. ^c LanL2DZ effective core potential was used for the core electrons of iodine and the valence electrons basis set coefficients were taken directly from ref 55. 6-31+G* was used for the carbon atom.

C. Calculations. Ab initio calculations were carried out for the ground state of the anion and both the singlet and triplet state of the neutrals to determine the geometries and vibrational frequencies for each system. For all of the dihalocarbenes, the anion state exhibits the largest C–X (X = F, Cl, Br, I) bond length and the smallest X–C–X angle in comparison to the corresponding neutral states. In CF_2 , that C–F bond length in the *singlet* state is slightly smaller ($\sim 1\%$) than that calculated for the triplet state. This is in agreement with calculations performed by Russo et al.¹³ On the other hand, the C–X bond length is smaller in the *triplet* state than in the singlet state for CCl_2 , CBr_2 , and CI_2 . The trend for the X–C–X angle is the same for all of the dihalocarbenes; the angle increases slightly from the anion to the singlet state and more substantially to the triplet state. All values are listed in Table 3. Two of the normal modes are totally symmetric and could be active in the photoelectron spectra: the C–X symmetric stretching (ν_1) and the X–C–X bending (ν_2) vibrations (see Table 4). The degree to which they are active depends on the displacement between corresponding modes in the anion and the neutral states.

The geometrical parameters and frequencies were used for Franck–Condon analysis to determine the relative intensities of the vibrational transitions expected in the photoelectron spectra (see section IV.B). The intensities are essential in determining the possibility of observing the 0–0 transition in the singlet and triplet states of the dihalocarbenes especially in the cases where there is a large geometry change and therefore a long vibrational progression.

IV. Discussion

A. Vibrational Frequencies. 1. Singlet State. The singlet state of CF_2 shows vibrational structure that is well resolved allowing for an accurate determination of both frequencies, ν_1 and ν_2 . Labeled in the top spectrum of Figure 1 with a filled circle, the symmetric stretch is approximately $1220 \pm 15 \text{ cm}^{-1}$, which is in very close agreement with the value of $1228 \pm 30 \text{ cm}^{-1}$ previously determined via photoelectron spectroscopy in this laboratory.⁴⁸ In addition, this value is consistent with the gas phase value, 1225.08 cm^{-1} , determined by Davies et al.,²⁵ and the matrix value,²² 1221 cm^{-1} . The bending frequency, marked with an asterisk in Figure 1, is determined to be $670 \pm 15 \text{ cm}^{-1}$. This value is slightly different from that measured previously by photoelectron spectroscopy, $706 \pm 30 \text{ cm}^{-1}$, but agrees well with the matrix value²² of 668 cm^{-1} . Additionally, calculations by Russo et al.¹³ predict values of 1196 and 634 cm^{-1} for the symmetric stretching and bending frequencies, respectively.

TABLE 4: Experimentally Determined Vibrational Frequencies for CX₂ (X = F, Cl, Br, I) in the Singlet ¹A₁ and Triplet ³B₁ States. Also Listed for Comparison Are Values Determined in Previous Experiments, Those Calculated Using MP2(FULL)/6-311+G*, and Those Predicted Previously^a

	CF ₂		CCl ₂		CBr ₂		Cl ₂	
	¹ A ₁	³ B ₁	¹ A ₁	³ B ₁	¹ A ₁	³ B ₁	¹ A ₁	³ B ₁
				ν_1				
expt								
this work	1220(15)	1020(3)	735(20)			525(20)		500(20)
other	1221 ^b		720 ^c		595 ^d			
theory								
this work	1254	1159	773	716	625	550	505 ^e	431 ^e
other	1196	1195	728	694	613	540		
				ν_2				
expt								
this work	670(15)	520(30)	340(20)			200(20)		120(20)
other ^f	668 ^b		327 ^c		196 ^d			
theory								
this work	680	522	357	315	206	192	142 ^e	136 ^e
other ^f	634	527	326	303	186	182		

^a ν_1 is the C–X symmetric stretch and ν_2 is the XCX bend. All values are in wavenumbers. Values in parentheses are error bars. ^b Reference 22. ^c Reference 34. ^d Reference 42. ^e LanL2DZ effective core potential was used for the core electrons of iodine and the valence electrons basis set coefficients were taken directly from ref 55. 6-31+G* was used for the carbon atom. ^f Reference 13.

Similarly, the singlet state of CCl₂ can be accurately assigned and vibrational frequencies can be extracted. In the bottom portion of Figure 1, the symmetric stretching frequency is measured to be $735 \pm 20 \text{ cm}^{-1}$, very close to the previous PES result⁴⁸ of $730 \pm 40 \text{ cm}^{-1}$ and the calculated frequency, 728 cm^{-1} . There is also agreement with the value determined from experiments in solid Ar, $\sim 720 \text{ cm}^{-1}$.^{32,35} The other prominent progression identifiable in the photoelectron spectrum of CCl₂⁻ is a progression of the symmetric stretch with one quantum of Cl–C–Cl bend, marked with an asterisk in Figure 1. This progression reveals a bending frequency of $340 \pm 20 \text{ cm}^{-1}$, the same value determined from PES earlier.⁴⁸ These values agree well with theory,¹³ 326 cm^{-1} , and experiment,³⁵ 333 cm^{-1} . In general, these measured vibrational frequencies are in agreement with our unscaled calculated values.

The singlet state in the CBr₂⁻ spectrum does not exhibit vibrational structure. A simulation using the unscaled values determined by our calculations, $\nu_1 = 625 \text{ cm}^{-1}$ and $\nu_2 = 206 \text{ cm}^{-1}$, reproduces the experimental spectrum after applying a full-width at half-maximum (fwhm) of 15 meV. These calculated frequencies agree well with those determined experimentally. Bondybey and English⁴² collected a spectrum of CBr₂ in solid Ar, obtaining 595 cm^{-1} for the C–Br symmetric stretching vibration and 196 cm^{-1} for the Br–C–Br bending vibration. Additionally, calculations by Russo et al.¹³ are also in close agreement, 613 and 186 cm^{-1} for ν_1 and ν_2 , respectively. The singlet state of Cl₂ is treated in a similar manner since there is very little vibrational resolution seen in the spectrum. Again, the vibrational frequencies from the calculations performed in this laboratory were used to simulate the spectrum. The spectrum is well reproduced with $\nu_1 = 505 \text{ cm}^{-1}$ and $\nu_2 = 142 \text{ cm}^{-1}$. Since there have been no previous studies on Cl₂, no comparisons can be made. A summary of some theoretical and experimental singlet state vibrational frequencies is in Table 4.

2. Triplet State. Considerably less information is known about the vibrational frequencies in the triplet states of CF₂, CCl₂, CBr₂, and Cl₂. To our knowledge, only theoretical calculations are available¹³ and this paper reports the first experimental measurements of these vibrational frequencies. For CF₂, the triplet state displays some vibrational resolution, shown in Figure 1, such that the frequencies may be measured. The main progression is assigned to the pure symmetric stretching vibration, resulting in $\nu_1 = 1020 \pm 30 \text{ cm}^{-1}$; this can be

compared to the calculated value of 1195 cm^{-1} .¹³ A less prominent progression is attributed to the bending mode at $520 \pm 30 \text{ cm}^{-1}$. For CCl₂, the triplet state in the bottom portion of Figure 1 reveals very little structure, making the experimental determination of frequencies impossible. Similar to the CBr₂ and Cl₂ singlet states, the frequencies from our calculations were used to simulate the CCl₂ triplet state. The values used were 715 and 315 cm^{-1} for ν_1 and ν_2 , respectively. They compare well with those determined using a higher level of theory as listed in Table 4.¹³

The triplet states of CBr₂ and Cl₂ (Figure 2) are the most prominent parts of the respective photoelectron spectra. Accurate determinations of the symmetric stretching frequencies for both CBr₂ and Cl₂ have been made. For CBr₂, $\nu_1 = 525 \pm 20 \text{ cm}^{-1}$ and for Cl₂, $\nu_1 = 500 \pm 20 \text{ cm}^{-1}$, these frequencies are marked with filled circles in Figure 2. The bending frequencies are more difficult to measure, giving $\nu_2 = 200 \pm 40$ and $120 \pm 40 \text{ cm}^{-1}$, for CBr₂ and Cl₂, respectively. The values for CBr₂ are in close agreement with theory,¹³ $\nu_1 = 540 \text{ cm}^{-1}$ and $\nu_2 = 182 \text{ cm}^{-1}$; however, there are no previous theoretical predictions for the Cl₂ system. In addition, estimates from our calculations provided a good template for these measurements. The outcome of these calculations is very close to those measured: ν_1 and ν_2 for CBr₂ and Cl₂ are 550 and 192 cm^{-1} and 430 and 135 cm^{-1} , respectively. These frequencies from the calculations performed in this laboratory have not been scaled. The experimental and unscaled calculated frequencies are found in Table 4.

B. Franck–Condon Analysis. Two different Franck–Condon analysis methods have been employed on the singlet and triplet states of the dihalocarbenes to aid in the identification of the 0–0 transition energies and to simulate the photoelectron spectra. In both methods, each state was simulated individually. The absolute energy was determined by aligning the VDE of the simulated spectrum to that of the experimental spectrum. The first method is the same as that previously used in this laboratory for the HCX (X = F, Cl, Br, I) halocarbenes.⁴⁸ The anion and neutral potential energy surfaces were assumed to be harmonic. The ab initio geometries were used as a guide; however, the change in geometry between the anion and the neutral was an adjustable parameter in order to match the breadth of the vibrational progression in the experimental spectrum. The simulations were generated by utilizing the measured frequencies (see section IV.A) or the ab initio frequencies for the states

with unresolved vibrational structure (Table 4) and a vibrational temperature of 300 K. Lastly, the fwhm was varied between 15 and 20 meV in order to match the widths of the experimental peaks. The addition of anharmonicity did not affect the quality of the simulations significantly. The simulations of the singlet and triplet states within each dihalocarbene were added together to obtain a total simulation of the experimental spectra. These simulations are shown with thin lines in Figures 1 and 2.

The second method for Franck–Condon analysis also has been implemented previously in this laboratory.⁵⁶ This method involves using a slightly modified version of the CDECK program.^{57,58} In this case, the normal modes and geometries from the calculations were also utilized but were not variable parameters when determining the Franck–Condon intensities and the breadth of the spectrum. Again, experimental frequencies were used when available, otherwise, the ab initio frequencies were used. A simulation of the photoelectron spectrum has been generated by convoluting the Franck–Condon transitions with Gaussians using a fwhm of 15–20 meV. These simulations are not shown in this paper; however, they do agree well with those shown in Figures 1 and 2.

From these Franck–Condon simulations, the origin transitions for both the singlet and triplet states have been obtained by extrapolating to lower electron binding energy. In addition, the relative intensities of the VDE (I_{VDE}) and the origin transition (I_{0-0}) have been determined for each state. In order to observe a peak in the spectrum assigned to the origin transition, the Franck–Condon factor for the 0–0 transition needs to be large enough relative to those for the higher energy transitions. This requires the geometries of the anion and neutral states to be relatively similar. For many systems, the geometry change is large so that it is impossible to detect the 0–0 transition. According to Franck–Condon analysis, the ratio $I_{\text{VDE}}:I_{0-0}$ is approximately 20:1 in the singlet states of CX_2 which is close to the signal-to-noise limit in the photoelectron spectra. As discussed in the previous section, the 0–0 transition for the CF_2 singlet state has been observed experimentally; however, those for CCl_2 , CBr_2 , and Cl_2 have not been. From the extrapolation, the origin transitions have been determined to be 1.59 ± 0.07 , 1.88 ± 0.07 , and 2.15 ± 0.07 eV for CCl_2 , CBr_2 , and Cl_2 , respectively. These energies are marked with solid arrows in Figures 1 and 2.

The triplet states of the dihalocarbenes were analyzed in a similar manner. The large differences in the anion and triplet state geometries result in a very low intensity 0–0 peak for CCl_2 , CBr_2 , and Cl_2 . It is predicted to be too small to be observed in the photoelectron spectrum with an average $I_{\text{VDE}}:I_{0-0}$ of approximately $10^5:1$. This is in contrast to CF_2 , which has a ratio of 20:1. After extrapolation, the 0–0 transition energies for the triplet states were determined to be 2.52 ± 0.12 , 1.71 ± 0.07 , 1.98 ± 0.07 , and 2.09 ± 0.07 eV for CF_2 , CCl_2 , CBr_2 , and Cl_2 , respectively. These energies are labeled with dashed arrows in Figures 1 and 2. From this analysis, it appears that the triplet state of Cl_2 is lower than the singlet state. The same was found true for HCl , which is thought to have a triplet ground state.⁵⁹ The origin transition energies of both the singlet and triplet states are listed in Table 5. The difference in the results from the two Franck–Condon analysis methods is included in the error bars.

C. Singlet–Triplet Splittings. Many theoretical studies on carbenes throughout the past several decades have concentrated on determining the singlet–triplet splitting energies for the dihalocarbenes.^{12–15} The level of theory that has been implemented to predict ΔE_{ST} has improved throughout the years.

TABLE 5: Origin Transition Energies of the Singlet and Triplet States of CF_2 , CCl_2 , CBr_2 , and Cl_2 ^a

transition	CF_2	CCl_2	CBr_2	Cl_2
$^1\text{A}_1(v=0) \leftarrow ^2\text{B}_1(v'=0)^b$	0.180(20)	1.59	1.88	2.15
$^3\text{B}_1(v=0) \leftarrow ^2\text{B}_1(v'=0)^b$	2.52(12)	1.71	1.98	2.09

^a All values are in electronvolts. Error bars are 0.07 eV unless otherwise noted in parentheses. ^b Values are obtained from simulations of the experimental spectra (see section IV.B for details).

TABLE 6: Singlet–Triplet Splitting Energies (ΔE_{ST}) for CX_2 ($\text{X} = \text{F}, \text{Cl}, \text{Br}, \text{I}$)^a

	CF_2	CCl_2	CBr_2	Cl_2
experiment				
this work ^b	54 ± 3	3 ± 3	2 ± 3	-1 ± 3
other ^c	56.6			
theory				
MP4 ^d	57.6	20.5	16.5	11.2
LCGTO-LSD/NLC ^e	54.1	23.4	18.5	15.3
LDA/NL ^f	55.6	23.8	22.4	16.5
DDCI ^g	56.3	19.7	15.6	
CCCI ^h	57.5	25.9		
DZP ⁱ			8.6	

^a Positive values indicate that the singlet state is more stable. All values are in kcal/mol. ^b Values are determined using the quantities found in Table 5. ^c References 29 and 30. ^d Reference 15. ^e Reference 13. ^f Reference 12. ^g Reference 14. ^h Reference 10. ⁱ Reference 6.

Although many experimental investigations have been performed on the neutral dihalocarbenes, few have focused on determining ΔE_{ST} . Until the present study, there has been only one experimental value for the ΔE_{ST} reported for any of the dihalocarbenes. An emission and energy transfer study of triplet CF_2 by Koda²⁹ in 1978 revealed a ΔE_{ST} for CF_2 of 56.6 kcal/mol. In 1988, Murray et al.⁴⁸ obtained a lower limit on the ΔE_{ST} for CF_2 of 50 kcal/mol using photoelectron spectroscopy; however a precise value was not possible due to low photon energies. The same PES experiment did not attempt to quantify the singlet–triplet splitting of CCl_2 .

To this point, only an approximation of the ΔE_{ST} has been reported using the measured vertical detachment energies. Using the origin transition energies listed in Table 5, revised singlet–triplet splitting energies have been determined to be 54 ± 3 , 3 ± 3 , 2 ± 3 , and -1 ± 3 kcal/mol for CF_2 , CCl_2 , CBr_2 , and Cl_2 , respectively. Again, the error bars include the discrepancy in the results from the different Franck–Condon analysis methods. These values and those determined through calculations are presented in Table 6. The calculations have been relatively successful at estimating the ΔE_{ST} for CF_2 with values ranging from 46.5 to 57.6 kcal/mol. The present value of 53.9 ± 3 kcal/mol is within error of the 56.6 kcal/mol obtained by Koda.²⁹ In comparison to CF_2 , the discrepancy between experiment and theory is large in the determination of ΔE_{ST} for CCl_2 , CBr_2 , and Cl_2 . For these dihalocarbenes, the experimental value is lower than that calculated by at least a factor of 4. For CCl_2 and CBr_2 where ΔE_{ST} is reported to be 3 ± 3 and 2 ± 3 kcal/mol, respectively, the theoretical values are between 10 and 32 kcal/mol. In the case of Cl_2 , we have found the triplet state to be approximately 1 ± 3 kcal/mol more stable than the singlet state, which is in contrast to all theoretical results that predict the singlet to be the lower state by 11.2–16.5 kcal/mol.^{12–15} In general, both the experimental and theoretical determinations conclude that the singlet–triplet splitting decreases from CF_2 to Cl_2 ; however, the experimental data suggest that the relative energies of the states may switch in the case of Cl_2 . In all cases, the CF_2 singlet–triplet splitting is the largest by a considerable amount.

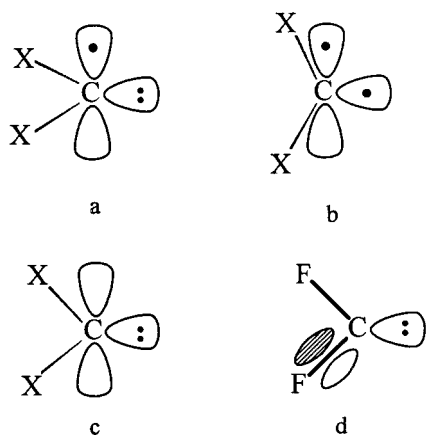


Figure 4. Orbital representations of the anion (a), triplet (b), and singlet (c) states of the CX_2 ($X = F, Cl, Br, I$) dihalocarbenes. Also shown (d) is a possible resonance structure for the singlet state of CF_2 .

As discussed above, the ΔE_{ST} of CF_2 is much greater than those determined for CCl_2 , CBr_2 , and Cl_2 . The theoretical predictions for ΔE_{ST} of CCl_2 , CBr_2 , and Cl_2 are too high even though the experimental values are based on extrapolated data and cannot be as accurately determined as would be possible with a well-resolved spectrum and smaller geometry changes between the anion and the neutral. For example, the calculated ΔE_{ST} for CCl_2 is, on average 20 kcal/mol (~ 0.9 eV) and the EA of CCl_2 is well determined at 1.59 eV.⁴⁸ A ΔE_{ST} of 0.9 eV would place the origin of the triplet state at 2.49 eV. According to the photoelectron spectrum in the bottom of Figure 1, this is clearly too high, falling near the peak of the triplet state portion of the spectrum. Given the overestimation of the ΔE_{ST} of CCl_2 , it is not surprising that there is similar discrepancy between the theoretical and experimental values for the more electron-rich species, CBr_2 and Cl_2 .

D. Stabilization Effects. It is useful to discuss the orbitals of the dihalocarbenes to better understand the relative energies of the singlet and triplet states. The anion ground state of the dihalocarbenes is a 2B_1 state and has the electronic configuration, $a_1^2b_1^1$, where a_1 has σ symmetry and b_1 is of π symmetry, giving $\sigma^2\pi^1$; both are nonbonding orbitals (see Figure 4a).^{11,12} The electronic configuration of the neutral state that is accessed upon photodetachment depends on the orbital from which the electron originated. Generally, the carbenes are electron deficient with two orbitals of relatively low energy that are competing for the same pair of electrons. Detachment of an electron from the σ orbital produces a triplet state (3B_1) in the neutral, leaving one valence electron in each of two nonbonding orbitals on the carbon atom, $\sigma^1\pi^1$ as illustrated in Figure 4b. If the electron in the π orbital is photodetached then the neutral is a singlet state, 1A_1 . Both nonbonding electrons are in the σ orbital, giving rise to a σ^2 electronic configuration, shown in Figure 4c. An electron can be detached from either orbital, yielding a photoelectron spectrum that contains features corresponding to transitions to both the singlet and triplet states as seen in Figures 1 and 2. It is not, however, obvious which will be the ground electronic state for each dihalocarbene and what will govern the relative stabilities of these states.

As discussed earlier, there is a large singlet state stabilization in CF_2 relative to the other dihalocarbenes. Several effects can dictate this singlet state stabilization. The F atom, with lone pairs in the p orbitals, preferentially binds to the p orbitals on carbon through π bonds. The F atom can withdraw electron density from the σ orbital and can donate it back to carbon through the π orbitals. This bonding will be the most favorable

with empty π orbitals on the carbon atom. Therefore, the stabilization will be the greatest in the singlet state when both electrons are in the σ orbital, resulting in the σ^2 configuration. This leads to the possibility of resonance structures in CF_2 . The good overlap between the p orbitals of the F and C atoms allows for the possibility of a partial double bond between the C and F atoms as illustrated in Figure 4d. The same arguments for the large singlet state stabilization in CF_2 can also be made for the destabilization of the CF_2 triplet state.

These stabilization effects are greatly reduced in the cases of Cl, Br, and I because of less favorable orbital overlap given the increase in the size of the substituent. An explanation as to why the triplet state may be the ground electronic state of Cl_2 also may be related to the size of the halogen substituent. As the size of the halogen substituent increases, the X–C–X angle also increases as seen in Table 3. As the angle approaches 180° , the triplet state will become more stable as the σ and π orbitals become equivalent.⁴

The energy of the origin transitions is also determined by the energy of the CX_2^- anion state. Therefore, comparisons of the relative energies of the states between the different carbenes are difficult to make. The anion stability is mainly determined by the electronegativity of the halogen substituent. However, other issues may affect the stability of the anion. In general, the stability should decrease from CF_2^- to Cl_2^- due to the decrease in the electronegativity. This stabilization effect would result in the largest origin transition energy for CF_2 and the smallest for Cl_2 . The origin transition energies, however, depend on the energies of both the neutral and the anion. There is a competition between the stabilization effects in the anion and neutral. As seen in Table 5, there is a trend to a less stable singlet state from CF_2 to Cl_2 indicating that the neutral state stabilization effects dominate the determination of the energy of the origin transition as is expected considering the same orbital argument.

The effects due to the change in the anion energy are canceled out when comparing the singlet–triplet splitting energies. The large stability of the singlet state with respect to the triplet state of CF_2 leads to the large ΔE_{ST} observed in the photoelectron spectrum. Consistent with the idea that the stabilization effects for the neutral singlet and triplet states are not as great in the other halogenated species, the ΔE_{ST} decreases sharply from CF_2 to CCl_2 and remains relatively constant for CBr_2 and Cl_2 .

V. Conclusions

Negative ion photoelectron spectra have been recorded for CF_2^- , CCl_2^- , CBr_2^- , and Cl_2^- using the 364 nm line from the output of an Ar ion laser. Vibrational transitions within both the ${}^1A_1 \leftarrow {}^2B_1$ and ${}^3B_1 \leftarrow {}^2B_1$ electronic transitions have been observed for all of the dihalocarbenes. Some of the states exhibit resolved vibrational structure enabling the determination of stretching and/or bending frequencies, all of which have been compared with other values.^{13,22,34,42} There is a clear dependence of the spectra on the laser polarization indicating that two different orbitals in the anion state are involved in the transitions to the neutral states resulting in a singlet and a triplet state.

Ab initio calculations have been carried out on the anion and neutral states. These results are utilized in Franck–Condon calculations to simulate the photoelectron spectra. From the simulations, the origin transition energies for the singlet and triplet states have been extracted allowing for the determination of the singlet–triplet splitting energies. A comparison of these values has been made with many theoretical calculations^{5,6,10,12–15} and experimental determinations.^{29,30} In the case of CF_2 , the

theoretical values are very close to the experimental value. This is in contrast to CCl_2 , CBr_2 , and Cl_2 where the theoretical values are much higher than those determined experimentally. CF_2 , CCl_2 , and CBr_2 all were determined to have singlet ground states but in the case of Cl_2 , the triplet state is probably the more stable state.

Acknowledgment. The work was supported by the National Science Foundation.

References and Notes

- (1) *Diradicals*; Borden, W. T., Ed.; Wiley: New York, 1982.
- (2) Skell, P. S. *Tetrahedron* **1985**, *41*, 1427.
- (3) Brahm, D. L. S.; Dailey, W. P. *Chem. Rev.* **1996**, *96*, 1585.
- (4) Tomioka, H. *Acc. Chem. Res.* **1997**, *30*, 315.
- (5) Bauschlicher, C. W., Jr.; Schaefer, H. F., III; Bagus, P. S. *J. Am. Chem. Soc.* **1977**, *99*, 7106.
- (6) Bauschlicher, C. W., Jr. *J. Am. Chem. Soc.* **1980**, *102*, 5492.
- (7) Ha, T.-K.; Gremlich, H.-U.; Buhler, R. E. *Chem. Phys. Lett.* **1979**, *65*, 16.
- (8) Nguyen, M. T.; Kerins, M. C.; Hegarty, A. F.; Fitzpatrick, N. J. *Chem. Phys. Lett.* **1985**, *117*, 295.
- (9) Carter, E. A.; Goddard, W. A., III *J. Phys. Chem.* **1986**, *90*, 998.
- (10) Carter, E. A.; Goddard, W. A., III *J. Phys. Chem.* **1987**, *91*, 4651.
- (11) Carter, E. A.; Goddard, W. A., III *J. Chem. Phys.* **1988**, *88*, 1752.
- (12) Gutsev, G. L.; Ziegler, T. *J. Phys. Chem.* **1991**, *95*, 7220.
- (13) Russo, N.; Sicilia, E.; Toscano, M. *J. Chem. Phys.* **1992**, *97*, 5031.
- (14) Garcia, V. M.; Castell, O.; Reguero, M.; Caballo, R. *Mol. Phys.* **1996**, *87*, 1395.
- (15) Gobbi, A.; Frenking, G. *J. Chem. Soc., Chem. Commun.* **1993**, 1162.
- (16) Mann, D. E.; Thrush, B. A. *J. Chem. Phys.* **1960**, *33*, 1732.
- (17) Bass, A. M.; Mann, D. E. *J. Chem. Phys.* **1962**, *36*, 3501.
- (18) Milligan, D. E.; Mann, D. E.; Jacox, M. E.; Mitsch, R. A. *J. Chem. Phys.* **1964**, *41*, 1199.
- (19) Powell, F. X.; Lide, D. R. *J. Chem. Phys.* **1966**, *45*, 1067.
- (20) Mathews, C. W. *Can. J. Phys.* **1967**, *45*, 2355.
- (21) Milligan, D. E.; Jacox, M. E. *J. Chem. Phys.* **1968**, *48*, 2265.
- (22) Bondybey, V. E. *J. Mol. Spectrosc.* **1976**, *63*, 164.
- (23) Lefohn, A. S.; Pimentel, G. C. *J. Chem. Phys.* **1971**, *55*, 1213.
- (24) King, D. S.; Schenck, P. K.; Stephenson, J. C. *J. Mol. Spectrosc.* **1979**, *78*, 1.
- (25) Davies, P. B.; Lewis-Bevan, W.; Russell, D. K. *J. Chem. Phys.* **1981**, *75*, 5602.
- (26) Davies, P. B.; Hamilton, P. A.; Elliott, J. M.; Rice, M. J. *J. Mol. Spectrosc.* **1983**, *102*, 193.
- (27) Suto, O.; Steinfeld, J. *Chem. Phys. Lett.* **1990**, *168*, 181.
- (28) Kirchhoff, W. H.; Lide, J., D. R.; Powell, F. X. *J. Mol. Spectrosc.* **1973**, *47*, 491.
- (29) Koda, S. *Chem. Phys. Lett.* **1978**, *55*, 353.
- (30) Koda, S. *Chem. Phys.* **1982**, *66*, 383.
- (31) Minton, T. K.; Felder, P.; Scales, R. C.; Huber, J. R. *Chem. Phys. Lett.* **1989**, *164*, 113.
- (32) Andrews, L. *J. Chem. Phys.* **1968**, *48*, 979.
- (33) Andrews, L.; Grzybowski, J. M.; Allen, R. O. *J. Phys. Chem.* **1975**, *79*, 904.
- (34) Tevault, D. E.; Andrews, L. *J. Mol. Spectrosc.* **1975**, *54*, 110.
- (35) Bondybey, V. E. *J. Mol. Spectrosc.* **1977**, *64*, 180.
- (36) Clouthier, D. J.; Karolczak, J. *J. Phys. Chem.* **1989**, *93*, 7542.
- (37) Choe, J.-I.; Tanner, S. R.; Harmony, M. D. *J. Mol. Spectrosc.* **1989**, *138*, 319.
- (38) Fujitake, M.; Hirota, E. *J. Chem. Phys.* **1989**, *91*, 3426.
- (39) Xu, S.; Harmony, M. D. *Chem. Phys. Lett.* **1993**, *205*, 502.
- (40) Andrews, L.; Carver, T. G. *J. Chem. Phys.* **1968**, *49*, 896.
- (41) Ivey, R. C.; Schultze, P. D.; Leggett, T. L.; Kohl, D. A. *J. Chem. Phys.* **1974**, *60*, 3174.
- (42) Bondybey, V. E.; English, J. H. *J. Mol. Spectrosc.* **1980**, *79*, 416.
- (43) Zhou, S. K.; Zhan, M. S.; Shi, J. L.; Wang, C. X. *Chem. Phys. Lett.* **1990**, *166*, 547.
- (44) Schlachta, R.; Lask, G.; Stangassinger, A.; Bondybey, V. E. *J. Phys. Chem.* **1991**, *95*, 7132.
- (45) Xu, S.; Harmony, M. D. *J. Phys. Chem.* **1993**, *97*, 7465.
- (46) Paulino, J. A.; Squires, R. R. *J. Am. Chem. Soc.* **1991**, *113*, 5573.
- (47) Poutsma, J. C.; Paulino, J. A.; Squires, R. R. *J. Phys. Chem.* **1997**, *101*, 5327.
- (48) Murray, K. K.; Leopold, D. E.; Miller, T. M.; Lineberger, W. C. *J. Chem. Phys.* **1988**, *89*, 5442.
- (49) Ervin, K. M.; Lineberger, W. C. Photoelectron Spectroscopy of Negative Ions. In *Advances in Gas-Phase Ion Chemistry*; Adams, N. G., Babcock, L. M., Eds.; JAI Press: Greenwich, CT, 1992; Vol. 1, p 121.
- (50) Neumark, D. M.; Lykke, K. R.; Anderson, T.; Lineberger, W. C. *Phys. Rev. A* **1985**, *32*, 1890.
- (51) Moore, C. E. *Atomic Energy Levels*; US GPO Circular No. 467; USGPO: Washington, DC, 1952.
- (52) Lee, J.; Grabowski, J. *J. Chem. Rev.* **1992**, *92*, 1611.
- (53) Cooper, J.; Zare, R. N. *J. Chem. Phys.* **1968**, *48*, 942.
- (54) Frisch, M. J.; Trucks, G. W.; Schlegel, H. B.; Gill, P. M. W.; Johnson, B. G.; Robb, M. A.; Cheeseman, J. R.; Kieth, T.; Petersson, G. A.; Montgomery, J. A.; Raghavachari, K.; Al-Laham, M. A.; Zakrewski, V. G.; Ortiz, J. V.; Foresman, J. B.; Cioslowski, J.; Stefanov, B. B.; Nanayakkara, A.; Challacombe, M.; Peng, C. Y.; Ayala, P. Y.; Chen, W.; Wong, M. W.; Andres, J. L.; Replogle, E. S.; Gomperts, R.; Martin, R. L.; Fox, D. J.; Binkley, J. S.; Defrees, D. J.; Baker, J.; Stewart, J. P.; Head-Gordon, M.; Gonzalez, C.; Pople, J. A. *Gaussian 94*, Rev. E.1; Gaussian, Inc.: Pittsburgh, PA, 1995.
- (55) Glukhovtsev, M. N.; Pross, A.; Radom, L. *J. Am. Chem. Soc.* **1995**, *117*, 2024.
- (56) Davico, G. E.; Schwartz, R. L.; Ramond, T. M.; Lineberger, W. C. *J. Am. Chem. Soc.* **1999**, *121*, 6047.
- (57) Chen, P. Unimolecular and Bimolecular Reaction Dynamics. In *Unimolecular and Bimolecular Reaction Dynamics*; Ng, C. Y., Baer, T., Powis, I., Eds.; John Wiley & Sons: New York, 1994.
- (58) We thank Peter Chen and Cameron Logan for providing us with a copy of their CDECK program.
- (59) Gilles, M. K.; Ervin, K. M.; Ho, J.; Lineberger, W. C. *J. Phys. Chem.* **1992**, *96*, 1130.